Corrosion Resistance and Tribological Characteristics of Polyaniline as Lubricating Additive in Grease

Zhengfeng Cao
School of Energy Power and Mechanical Engineering,
North China Electric Power University,
Beijing 102206, China
e-mail: czf90@ncepu.edu.cn

Yanqiu Xia[1]
School of Energy Power and Mechanical Engineering,
North China Electric Power University,
Beijing 102206, China;
State Key Laboratory of Solid Lubrication,
Lanzhou Institute of Chemical Physics,
Chinese Academy of Sciences,
Lanzhou 730000, China
e-mail: xiayq@ncepu.edu.cn

Polyaniline (PANI) was doped as lubricating additive to afford grease. The effect of PANI on the physicochemical characteristics, corrosion resistance, and tribological performances of lubricating grease was investigated in details, and the tribological action mechanisms of lubricating grease were analyzed in relation to worn surface analyses by scanning electron microscopy (SEM) and energy dispersive X-ray spectroscope (EDS). Results indicate that the PANI-doped grease has superior conductive and thermal properties. And PANI-doped grease has an excellent corrosion resistance, which is attributed to the isolation effect and the compact passivated film generated by reaction of PANI and metal. In the meantime, the PANI-doped grease performs superior friction reduction and wear resistance under different applied loads and frequencies. It is mainly ascribed that the PANI can perform like spacers to avoid direct contact between the contact interfaces, and the protective tribofilm is generated by physical adsorption and chemical reaction.
[DOI: 10.1115/1.4036271]

1 Introduction

Transmission line plays an important role in current transmission, and its reliable operation has attracted intensive attention across the industry and academia [1–4]. Transmission line often runs in atrocious environment including high/lower temperature, serious pollution, salt atmosphere, friction, and wear generated by vibration [5–8]. These factors make negative effects in reliability and service life. The abovementioned problems existing in transmission line, fortunately, could be overcome by introducing lubricating grease into the transmission line. When lubricating grease is applied in this situation, it should achieve the levels of excellent tribological performances to reduce frictional losses and wear, high thermal conductivity to dissipate the joule heat, and novel anticorrosion property to protect the transmission line. At present, current commercial lubricating grease applied in transmission line is prepared by adding multiple additives including anticorrosion, friction modifiers, antiwear, and thermal conductivity additives. Nevertheless, using multiple additives leads to the complexity of grease preparation process and the increase in cost, and partial performances such as tribological performances, thermal conductance, or anticorrosion property of current lubricating grease cannot meet the requirements. This leads to frequent failures in transmission line.

Polyaniline is commonly identified to be one of the most potential conducting polymers for extensive applications, owing to its unique performances including ease of availability and synthesis, novel environment stability, relatively low cost, tunable electrical conductivity, and interesting redox characteristics associated with the chain nitrogen [9,10]. The structure of PANI can be illustrated by the general formula $[(—B—NH—B—NH—)_n\ (—B—N{=}Q{=}N—)_{1-n}]_m$, in which B and Q represent the rings in the benzenoid and quinonoid forms, respectively [11,12]. PANI has three oxidation states: the fully reduced form-leucoemeraldine ($n = 1$), the partially oxidized polymer-emeraldine ($n = 0.5$), and the fully oxidized form-pernigraniline ($n = 0$). Among the three types of oxidation states, the partially oxidized polymer-emeraldine (green color) is the most stable and exhibits an outstanding conductivity [13,14].

According to the *WEB of Science*, about 20,000 papers have been published in the past three decades on the application of PANI emerging in chemistry, material science, polymer science, and engineering. For example, it has been reported that the PANI could be used as substrates for light-emitting devices, the electrode in the battery, the composite coatings, etc. [15–18]. PANI has been also widely explored as anticorrosion coating for stainless steel [19–21], mild steel [22,23], copper [24,25], aluminum, and magnesium [26–28]. In addition, Dominis et al. [29] and Talo et al. [30] all concluded that the emeraldine base coating performed a better corrosion protection than other two PANI (leucoemeraldine and pernigraniline). Although numerous groups have investigated the wide application of PANI, there is rare paper about PANI used as lubricating additive. Therefore, considering the characteristics of PANI including commercial availability, high conductivity, anticorrosion protection, and environment stability, PANI is doped as lubricating additive to afford new grease. In the meantime, dinonyl-naphthalenesulfonic acid barium salt (T705), benzotriazole (T706), and graphite are selected as the contrastive additives. The physicochemical characteristics, anticorrosion property, and tribological performances of the prepared greases are investigated in details, and the tribological mechanisms are analyzed in relation to worn surface analyses by SEM and energy dispersive EDS.

2 Experimental Details

2.1 Materials. The base oil obtained from Nanjing Golden Chemical Co., Ltd., (Nanjing, China) is a kind of oil soluble polyether (denoted as OSP 680), and its main characteristics are listed in Table 1. Lithium hydroxide, sebacic acid, 12-hydroxystearic acid, and PANI (density: 0.4 g/cm^3 and grain size: 1–2 μm) are purchased from Sinopharm Chemical Reagent Co., Ltd., (Beijing, China). T705, T706, and graphite provided by Zhongcheng Petrochemical Co., Ltd., (Changsha, China) are introduced as lubricating additives for comparative study, Fig. 1 is the structural formula of T705 and T706, and Table 2 lists their main characteristics. The

[1]Corresponding author.
Contributed by the Tribology Division of ASME for publication in the JOURNAL OF TRIBOLOGY. Manuscript received September 23, 2016; final manuscript received February 18, 2017; published online June 30, 2017. Assoc. Editor: Ning Ren.

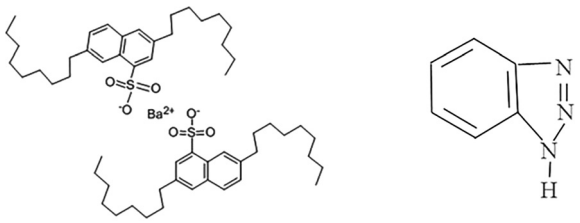

Fig. 1 Structural formula of T705 and T706

Table 1 Main characteristics of the oil soluble polyether (OSP 680)

Item	OSP 680	Standard
Kinematic viscosity (cS) 40 °C	680	ASTM D445
Kinematic viscosity (cS) 100 °C	77	ASTM D445
Viscosity index	196	ASTM D2270
Pour point (°C)	−30	ASTM D97
Flash point (°C)	243	ASTM D92
Fire point (°C)	270	ASTM D92
Aniline point (°C)	<−30	ASTM D611-01

Table 2 Typical properties of T705, T706, and graphite

Item	T705	T706	Graphite
State of matter 25 °C	Liquid	Solid	Solid
Purity (%)	>99	>99	>98
Moisture content (%)	<0.1	<0.1	<0.1
Ash content (%)	<0.05	<0.05	<0.1
PH	5	5.5	—

PANI is also characterized using scanning electron microscope and Fourier transform infrared spectrometer (FT-IR spectrometer), and Fig. 2 affords the SEM morphology and characteristic spectrum.

In the curve of the PANI powder, the peaks at about 1560 cm^{-1} and 1470 cm^{-1} are assigned to the stretching vibration of the quinoid (Q) and benzenoid (B) rings [31,32]. The almost equal intensity of these two peaks demonstrates that the PANI could be in the polyaniline emeraldine state [33]. The peak at 1301 cm^{-1} is related to the C–N stretching of a secondary aromatic amine. The aromatic C–H in-plane bending modes are usually observed from the band at around 1132 cm^{-1}. The peaks at 887 cm^{-1} and 813 cm^{-1} are attributed to the aromatic C–H out-of-plane bending mode [31]. The FT-IR absorption spectroscopy shows that the PANI powder is polyaniline in emeraldine state [34].

2.2 Preparation of the Lubricating Greases. The complex lithium-based grease was synthesized according to two-step method. First, pure OSP 680 (50%, mass fraction, the same hereafter) and 12-hydroxystearic acid (7.87%) were infused into the correlative vessel and started to agitate right now. The temperature of mixture was raised to 80° C to dissolve 12-hydroxystearic acid. Second, the reaction temperature was raised to 100° C, and a certain aqueous solution of lithium hydroxide monohydrate (1.12%) was introduced into the vessel under 1 h of agitation. Third, the surplus base oil (38%), sebacic acid (2.11%), and equivalent aqueous solution of lithium hydroxide monohydrate (0.9%) were slowly injected into the vessel, and the reaction temperature was raised to 210° C for 10 mins. Fourth, the resultant mixture was cooled down to 50° C, and a certain amount of lubricating additives (0.5%, 1.0%, 1.5%, 2.0%, and 2.5%) was slowly poured into the vessel under another 30 mins of agitation. Finally, the mixture was cooled to room temperature (RT) and rolled on a three-roller mill to afford the target products.

2.3 Characterization of the Lubricating Greases. The penetration, dropping point, and copper strip tests of the lubricating greases were investigated according to national standards, including GB/T 269, GB/T 3498, and GB/T 7326, respectively. The surface volume resistivity and thermal conductivity of lubricating greases were measured with GEST-121 surface volume resistivity meter and TC3000E thermal conductivity instrument at room temperature, respectively. Thermogravimetric analyses (TGA) of the lubricating greases were carried out on a Q500 TGA (TA Instruments, New Castle, DE) at a heating rate of 10° C min^{-1} in air. And the anticorrosion performances were evaluated with YWX/Q-250B salt spray test instrument (Aimosheng, Jiangsu, China) according to national standard GB/T 2423.

2.4 Friction and Wear Tests. The MFT-R4000 reciprocal friction and wear apparatus was performed to evaluate the tribological characteristics of as-synthesized lubricating greases in a ball-on-block configuration. The commercially upper ball (AISI 52100 steel ball, diameter 5 mm, and hardness 710 Hv) was driven to reciprocally slide against the lower block (Φ24 × 7.9 mm, 2024 aluminum, hardness 160–170 Hv, and surface roughness 0.05 μm) at the amplitude of 5 mm and an ambient temperature of ∼25° C for a duration of 30 mins. Before and after each sliding test, the upper ball and the lower block were ultrasonically washed with petroleum ether for 15 mins. Prior to sliding, approximately 1 g of the to-be-tested grease was introduced into the contact zone of the sliding pair. The tribological test parameters including applied loads and frequencies range from 30 N to 45 N (∼1.44 GPa–1.65 GPa) and 2 Hz to 5 Hz, respectively. The sliding test under each preset

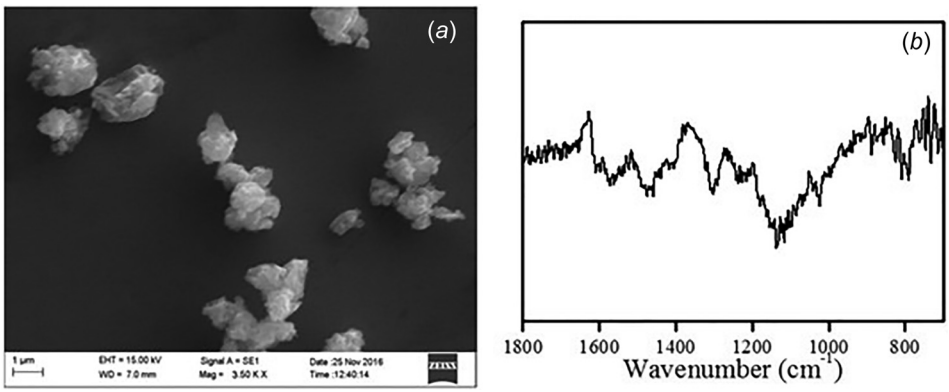

Fig. 2 SEM morphology and Fourier transform infrared analysis spectra of PANI

Table 3 Physicochemical properties of the several lubricating greases

Sample	Base grease	PANI (1.5%) grease	T705 (2.0%) grease	T706 (1.5%) grease	Graphite (1.5%) grease
Dropping point (°C)	270	306	275	268	287
Penetration (0.1 mm)	279	256	284	289	263
Copper corrosion (T2copper, 100 °C, 24 h)	1a	1a	1a	1a	1a
Surface volume resistivity (Ω cm)	4.7×10^{12}	1.3×10^{12}	5.1×10^{12}	4.9×10^{12}	1.7×10^{12}
Thermal conductivity (W/m K)	0.27	0.34	0.26	0.26	0.33

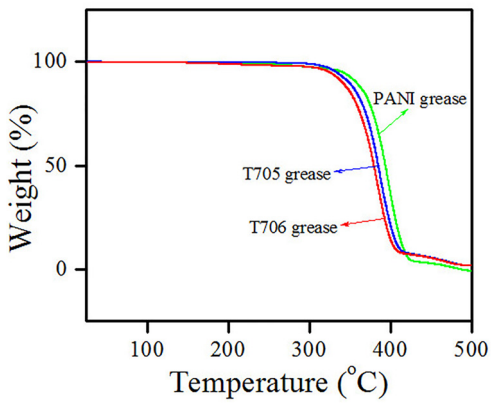

Fig. 3 TGA curves of the lubricating greases

condition was repeated three times to minimize data scattering. The mean values of the coefficient of friction (COF) and wear width are provided in association with error bars in this paper. The morphologies and chemical composition of the worn surfaces were analyzed with the EVO-18 SEM (Zeiss, Jena, Germany) and energy dispersive X-ray spectroscopy (EDS, Bruker, Karlsruhe, Germany).

3 Results and Discussion

3.1 Properties of the Lubricating Greases

3.1.1 Physicochemical Characteristics of Lubricating Greases. The physicochemical characteristics of the grease can be used to demonstrate the fundamental properties. According to the tribological tests shown in the following passage, we provide physicochemical properties of the as-synthesized greases which contain 1.5% PANI, 2.0% T705, 1.5% T706, and 1.5% graphite in Table 3, respectively. The results indicate that the PANI has great influence on the dropping point and penetration of the base grease. The reason might lie in that PANI has a high special surface area (SSA) and can retard the transfer of liquid molecules, thereby leading to high dropping point and low penetration [35]. In the meantime, due to the excellent conductivity and high SSA of PANI, which make a positive contribution to forming more contact points in lubricating grease [36–38], the PANI grease performs a lower surface volume resistivity and a higher thermal conductivity.

3.1.2 Thermal Stability of the Lubricating Grease. Figure 3 shows the thermal gravimetric analysis curves of the lubricating greases. It can be observed that the decomposition temperature of PANI grease is only a little higher than the other two greases, demonstrating that lubricating additive has little effect on the high thermal stability of the lubricating greases.

3.1.3 Corrosion Resistance of the Lubricating Greases. The corrosion resistance of the as-synthesized greases for steel and aluminum was evaluated with YWX/Q-250B salt spray test instrument according to national standard GB/T 2423. The test was conducted at the temperature of 35° C ± 1° C and the NaCl concentration of 5% ± 0.1% for a duration of 480 h.

The aluminum and steel blocks after salt spray test were shown in Fig. 4. All the aluminum and steel blocks covered with T705, T706, and PANI greases were smooth and bright without any corrosion spot. In a sharp contrast, the aluminum and steel blocks covered with base and graphite greases were corroded. This test indicates that the PANI dispersed in grease also performed an excellent anticorrosion property as same as the anticorrosion additives (T705 and T706). The excellent anticorrosion performance of PANI-doped grease might lie in that the blocks covered with PANI-doped grease can be isolated from most of O_2, H_2O, and other corrosive materials, and at the same time PANI possessing

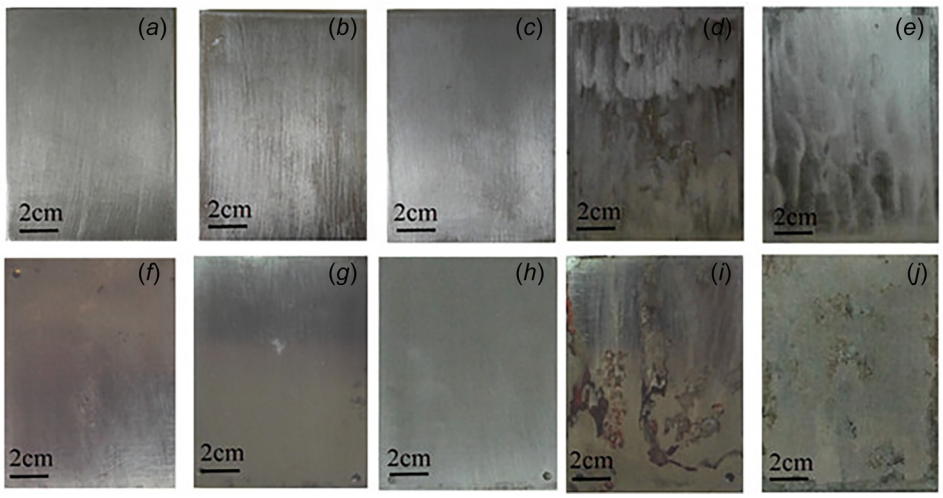

Fig. 4 Aluminum and steel blocks after salt spray test. (*a*) and (*a*′) PANI grease, (*b*) and (*b*′) T705 grease, (*c*) and (*c*′) T706 grease, (*d*) and (*d*′) graphite grease, and (*e*) and (*e*′) base grease (upper blocks are aluminum and lower blocks are steel).

high oxidation–reduction potential can react with Fe to form a dense passivation film in the presence of water and oxygen. The reaction can be explained by the equation [39–42]

$$Fe + 3PANI^{+} + 3H_2O = Fe(OH)_3 + 3PANI + 3H^{+}$$

Since Al has a lower oxidation–reduction potential and more active properties than Fe, Al can also undergo a similar reaction. Therefore, PANI-doped grease exhibits an excellent corrosion resistance. Due to the poor anticorrosion performance of graphite grease, the influence of load and frequency in tribological performances for graphite grease is not investigated any more in following passage.

3.2 Tribological Test Results. To evaluate the tribological performances of the lubricating additives, this article investigated three predominant factors (additive concentration, load, and frequency).

3.2.1 Influence of Additive Concentration in Tribological Performances. Figure 5 reveals the evolution of COFs and wear widths of the aluminum disk under the lubricating of greases doped with various additives (load: 30 N, frequency: 5 Hz, and room temperature). It can be seen that the PANI can effectively improve the tribological characteristics of the base grease. The PANI-doped grease (additive content: 1.5%) exhibits lowest COF (0.097) and wear width (0.389 mm) among all the greases. At the same time, it can be clearly observed that the various lubricating greases with addition of 2.0% T705, 1.5% T706, and 1.5% graphite exhibit better tribological properties. Therefore, in following experiments, the concentration of PANI, T705, T706, and graphite in grease would be 1.5%, 2.0%, 1.5%, and 1.5%, respectively.

3.2.2 Influence of Load in Tribological Performances. Figure 6 presents the mean COFs and wear widths of the steel–aluminum sliding pair under grease lubrication at various loads (5 Hz, RT). It is seen that all the additives are favorable for reducing the COFs, and the COFs and wear widths tend to rise with increasing load. The mean COFs of PANI-doped grease are between 0.096 and 0.11, and they are smaller than those of base grease (0.11–0.127), T705 grease (0.107–0.125), and T706 grease (0.101–0.12) at the same load. This reveals that the PANI-doped grease exhibits a better friction reducing ability than other greases. Meanwhile, the wear widths of the lubricating greases increase as follows: PANI < T706 < T705 < base grease, which shows that the PANI-doped grease has a better antiwear ability than T705 and T706 greases.

3.2.3 Influence of Frequency in Tribological Performances. Figure 7 shows the mean COFs and wear widths of the aluminum disk lubricated by greases at various frequencies (40 N, RT). It is obviously seen that the COFs (0.09–0.096) and wear widths (0.433–0.456 mm) of PANI-doped grease are smaller than those of other greases (all above 0.108 and 0.518 mm) at various frequencies. Compared with base grease, the biggest reduction of PANI-doped grease in COF and wear width is about 25.6% and 29%, respectively. The results demonstrate that the PANI-doped grease performs a better friction reducing and wear resistance ability than other greases.

3.2.4 Friction Test With Current. The MFT-R4000 reciprocating friction and wear tester (Fig. 8(*a*)) was employed to continue evaluating tribological performance of lubricating greases with current. Figure 8(*b*) shows the evolution of friction coefficient with time during a current ramp test from 0 to 20 A at room temperature (load: 20 N and frequency: 5Hz). As shown in Fig. 8(*b*), during the first 10 min of friction test, the friction coefficient of all the greases was stable. After current was loaded, the friction coefficient of PANI-doped grease is the lowest during the full current range. When the current is 10 A, the friction coefficient of base grease is still stable and shows no obvious change; the friction coefficient of T705-doped grease and T706-doped grease is not stable and goes a little higher; and the friction coefficient of PANI-doped grease drops a little. When the current is 20 A, the friction coefficient of base grease and T705-doped grease is not stable and going up; the friction coefficient of T706-doped grease and PANI-doped grease has a small fluctuation, but the friction coefficient of PANI-doped grease is still lowest. It is presumed that the reduction in friction coefficient of PANI grease

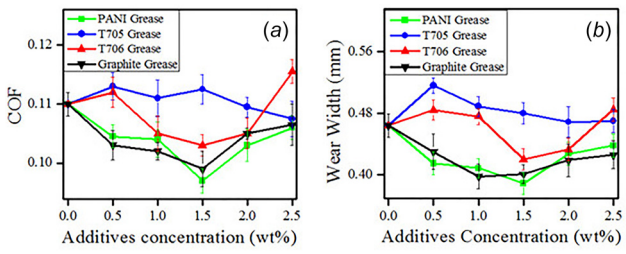

Fig. 5 Evolution of average COFs (*a*) and average wear widths (*b*) for the prepared greases at different additives concentration at RT

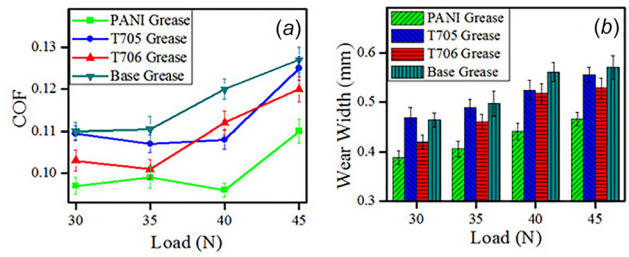

Fig. 6 Evolution of average COFs (*a*) and average wear widths (*b*) for the prepared greases at different loads, 5 Hz, and RT

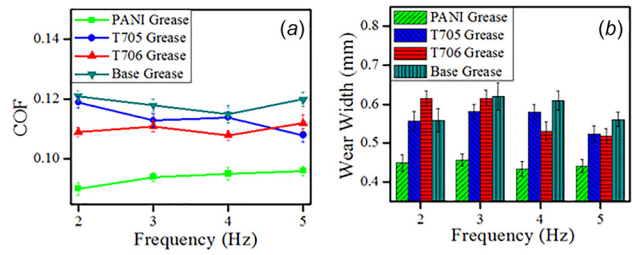

Fig. 7 Evolution of average COFs (*a*) and average wear widths (*b*) for the prepared greases at different frequencies, 40 N, and RT

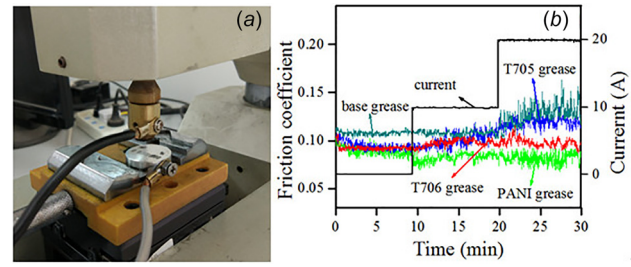

Fig. 8 MFT-R4000 tribometer and evolution of friction coefficient with time during a current ramp test from 0 to 20 A for PANI grease at room temperature (load: 20 N, stroke: 5 mm, frequency: 5 Hz, and current: 0–20 A)

is dominated by two reasons. One is that when the current is loaded, the conductive PANI particles existing between friction pairs can be adsorbed on the worn surface to form an adsorption film, and the other one is that although the heat produced by electric current and friction goes against the formation of lubricating oil film, it promotes PANI to react with friction pairs to form a protective tribofilm. Therefore, PANI grease performs superior tribological performances at current carrying condition.

3.3 Analysis of the Worn Surfaces. The surface morphologies of the worn surfaces on the lower aluminum blocks lubricated by the grease doped with various additives are provided in Fig. 9 (40 N and 5 Hz). All the surface morphologies are obtained in the same conditions. It can be seen that the worn surfaces of the aluminum blocks lubricated with T705 and T706 greases are relatively rough and contain dense furrows and large pits (Figs. 9(*b*), 9(*c*), 9(*b*′), and 9(*c*′)). Different from the abovementioned, the worn surface lubricated by PANI-doped grease contains a little shallow furrows and it is much narrower and smoother (Figs. 9(*a*) and 9(*a*′)), which well corresponds to the better antiwear ability of PANI than other additives.

Energy dispersive X-ray spectroscope is a powerful experimental facility to characterize the typical elements on worn surfaces. Figure 10 provides the EDS spectra of some typical elements on the steel ball and lower aluminum block lubricated with base grease and PANI grease at 40 N and 5 Hz. The content of N and C elements on the worn surfaces lubricated by PANI-doped grease is obviously higher than that of N and C elements on the worn surfaces lubricated by base grease. These elements have a crucial influence in the friction reducing and antiwear performances. It is presumed that a denser and more sufficient protective tribofilm is generated by the complex physical and chemical reaction.

The lubricating effectiveness and performance of solid lubricants depend on the optimal concentration and the surface protective film, respectively. Figure 11 is a schematic diagram of PANI dispersing in the lubricating greases in the sliding process, and the good tribological characteristics of PANI as lubricating additive of grease can be explained as follows. First, PANI powders existing between the friction pair can increase the contact area of the steel–aluminum pair, thereby performing like spacers to avoid direct contact between the contact interfaces [43,44]. Second, during the sliding process, friction surfaces are easy to lose electrons,

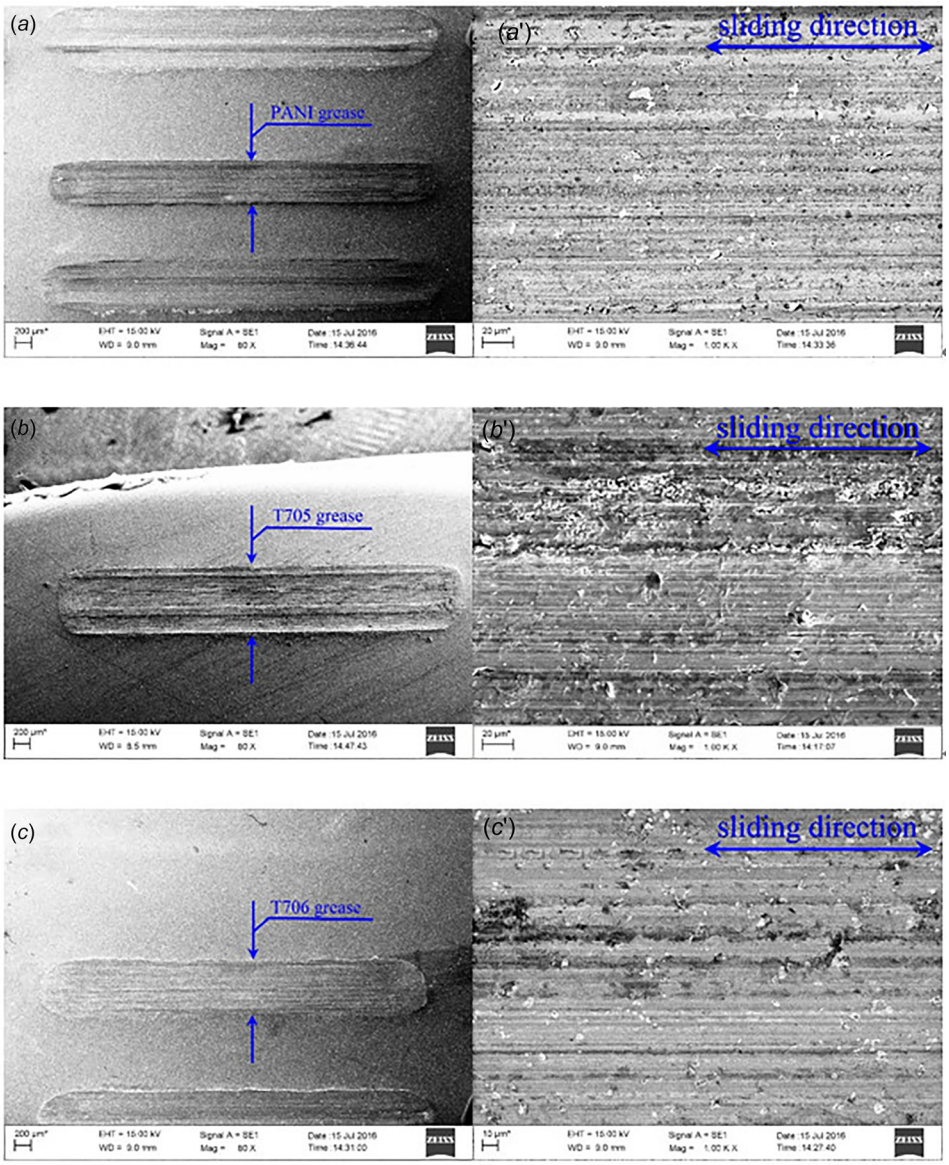

Fig. 9 Morphologies of the worn surfaces lubricated with lubricating greases at 40 N and 5 Hz. (*a*) and (*a*′) PANI grease, (*b*) and (*b*′) T705 grease, and (*c*) and (*c*′) T706 grease.

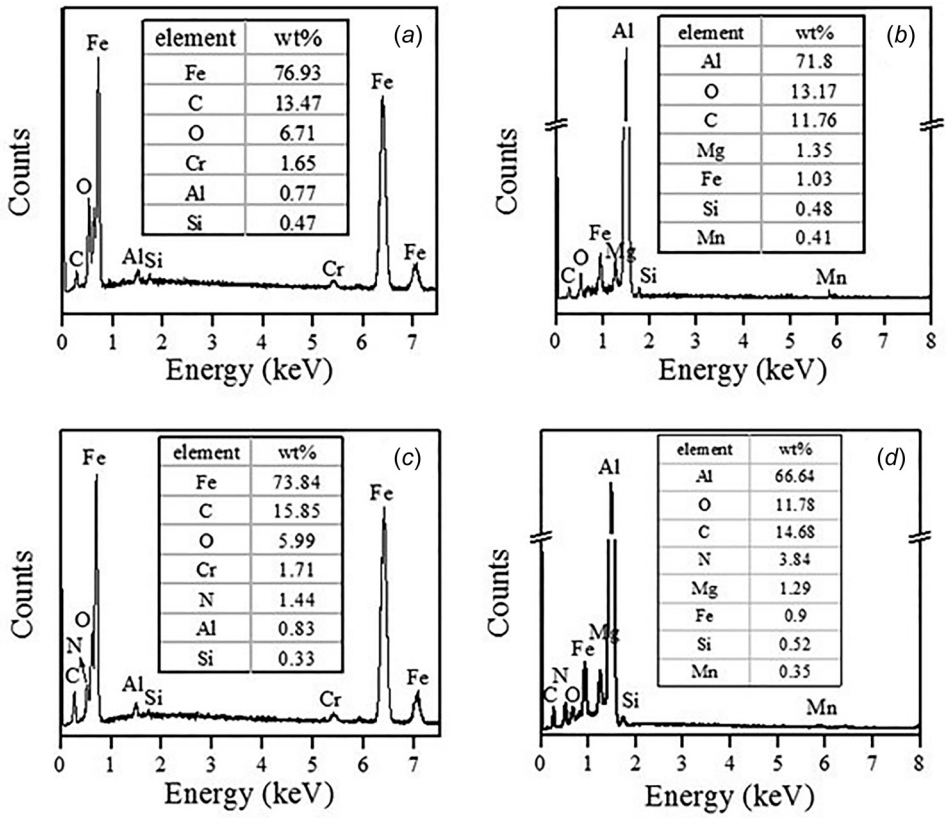

Fig. 10 EDS of the worn surfaces lubricated with base and PANI greases at 40 N and 5 Hz. Base grease: (*a*) steel ball and (*b*) aluminum block; and PANI grease: (*c*) steel ball and (*d*) aluminum block.

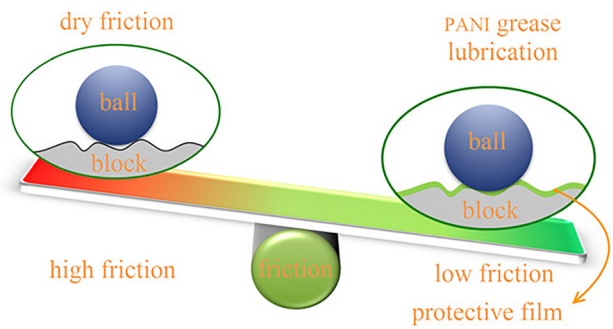

Fig. 11 Schematic of friction mechanism of PANI greases

leading a large number of small particles such as C and PANI particles to be absorbed on the worn surfaces, thereby improving antiwear ability. Third, PANI can react with metal to generate a compact passivated film, and oxidation reaction also occurs on worn surface to form a metallic oxide film. Thus, the protective film possessing the ability of friction reducing and antiwear properties is formed on the friction surfaces to promote the tribological performances [36,45].

4 Conclusions

The conclusions summarize the above experimental works of lubricating greases as follows: the polyaniline (PANI, emeraldine state) as lubricating additive in grease is able to greatly improve the conductivity, thermal property, and corrosion resistance of base grease. The excellent corrosion resistance is attributed to the isolation effect and the compact passivated film generated by reaction of PANI and metal. Besides, the PANI as lubricating additive can also improve the friction reduction and antiwear abilities of base grease, and the optimal concentration for PANI is recommended as 1.5%. The reasons lie in that the PANI can perform like spacers to avoid direct contact between the contact interfaces, and the protective tribofilm is generated by physical adsorption and chemical reaction. This paper provides a direction for application of PANI, and due to the excellent performances of PANI-doped grease, it is expected that the PANI could have potential application as a lubricant for the industry.

Funding Data

- National Natural Science Foundation of China (Grant No. 51575181).

References

[1] Mcelvain, F. R., and Mulnix, S. S., 2000, "Statistically Determined Static Thermal Ratings of Overhead High Voltage Transmission Lines in the Rocky Mountain Region," IEEE Trans. Power Syst., **15**(2), pp. 899–902.

[2] Nikiforov, E. P., 2004, "Raising the Reliability of Overhead Transmission Lines Under the Action of Atmospheric Loads," Hydrotech. Constr., **38**(1), pp. 49–53.

[3] Wei, Y., Yang, Q., Xiong, X., Wang, J., and Weng, S., 2014, "Short-Term Reliability Evaluation of Transmission System Under Strong Wind and Rain," J. Power Energy Eng., **2**(4), pp. 665–672.

[4] Liu, W. X., Xu, J. K., Jiang, H. Y., and Shen, Y. T., 2013, "Reliability Parameters Forecasting for Transmission Lines Based on Principal Component Regression," Appl. Mech. Mater., **291–294**, pp. 2381–2386.

[5] Kopsidas, K., and Rowland, S. M., 2009, "A Performance Analysis of Reconductoring an Overhead Line Structure," IEEE Trans. Power Delivery, **24**(4), pp. 2248–2256.

[6] Harvard, D. G., Bellamy, G., Buchan, P. G., and Ewing, H. A., 1992, "Aged ACSR Conductors. I. Testing Procedures for Conductors and Line Items," IEEE Trans. Power Delivery, **7**(2), pp. 581–587.

[7] Deng, Y. J., Yu, J. C., Xia, K. Q., and Yang, L., 2013, "Corrosion Conditions Analysis of In-Service ACSR Overhead Lines," Appl. Mech. Mater., **446–447**, pp. 753–758.

[8] Fadel, A. A., Rosa, D., Murça, L. B., Fereira, J. L. A., and Araujo, J. A., 2011, "Effect of High Mean Tensile Stress on the Fretting Fatigue Life of an Lbis Steel Reinforced Aluminium Conductor," Int. J. Fatigue, **42**(4), pp. 24–34.
[9] Chang, K. C., Yeh, J. M., Lai, M. C., Peng, C. W., Chen, Y. T., and Lin, C. L., 2006, "Comparative Studies on the Corrosion Protection Effect of DBSA-Doped Polyaniline Prepared From In Situ Emulsion Polymerization in the Presence of Hydrophilic Na^+-MMT and Organophilic Organo-MMT Clay Platelets," Electrochim. Acta, **51**(26), pp. 5645–5653.
[10] Bhadra, S., Khastgir, D., Singha, N. K., and Lee, J. H., 2009, "Progress in Preparation, Processing and Applications of Polyaniline," Prog. Polym. Sci., **34**(8), pp. 783–810.
[11] Palaniappan, S., and John, A., 2008, "Polyaniline Materials by Emulsion Polymerization Pathway," Prog. Polym. Sci., **33**(7), pp. 732–758.
[12] Jaymand, M., 2013, "Recent Progress in Chemical Modification of Polyaniline," Prog. Polym. Sci., **38**(9), pp. 1287–1306.
[13] Kraljić, M., Mandić, Z., and Duić, L., 2003, "Inhibition of Steel Corrosion by Polyaniline Coatings," Corros. Sci., **45**(1), pp. 181–198.
[14] Cochet, M., Buisson, J. P., Wéry, J., Jonusauskas, G., Faulques, E., and Lefrant, S., 2001, "A Complete Optical Study of the Conductive Form of Polyaniline: The Emeraldine Salt," Synth. Met., **119**(1–3), pp. 389–390.
[15] He, Y., Wang, J. A., Zhang, W., Song, J., Pei, C., and Chen, X., 2010, "ZnO-Nanowires/PANI Inorganic/Organic Heterostructure Light-Emitting Diode," J. Nanosci. Nanotechnol., **10**(11), pp. 7254–7257.
[16] Lee, B. H., Back, H. C., Park, S. H., and Lee, K., 2009, "Flexible Polymer Electronic Devices Using Highly Conductive Polyaniline Electrode," Proc. SPIE-Int. Soc. Opt. Eng., **7416**(4), pp. 285–300.
[17] Wang, H. L., Macdiarmid, A. G., Wang, Y. Z., Gebier, D. D., and Epstein, A. J., 1996, "Application of Polyaniline (Emeraldine Base, EB) in Polymer Light-Emitting Devices," Synth. Met., **78**(1), pp. 33–37.
[18] Jing, X., and Wang, Y., 2004, "Preparation of an Epoxy/Polyaniline Composite Coating and Its Passivation Effect on Cold Rolled Steel," Polym. J., **36**(5), pp. 374–379.
[19] Zhong, L., Zhu, H., Hu, J., Xiao, S., and Gan, F., 2006, "A Passivation Mechanism of Doped Polyaniline on 410 Stainless Steel in Deaerated H_2SO_4 Solution," Electrochim. Acta, **51**(25), pp. 5494–5501.
[20] Shabani-Nooshabadi, M., Ghoreishi, S. M., Jafari, Y., and Kashanizadeh, N., 2014, "Electrodeposition of Polyaniline-Montmorrilonite Nanocomposite Coatings on 316L Stainless Steel for Corrosion Prevention," J. Polym. Res., **21**(4), pp. 1–10.
[21] Le, D. P., Yoo, Y. H., Kim, J. G., Cho, S. M., and Son, Y. K., 2009, "Corrosion Characteristics of Polyaniline-Coated 316L Stainless Steel in Sulphuric Acid Containing Fluoride," Corros. Sci., **51**(2), pp. 330–338.
[22] Jadhav, R. S., Hundiwale, D. G., and Mahulikar, P. P., 2010, "Synthesis of Nano Polyaniline and Poly-*O*-Anisidine and Applications in Alkyd Paint Formulation to Enhance the Corrosion Resistivity of Mild Steel," J. Coat. Technol. Res. **7**(7), pp. 449–454.
[23] Lu, W. K., Elsenbaumer, R. L., and Wessling, B., 1995, "Corrosion Protection of Mild Steel by Coatings Containing Polyaniline," Synth. Met., **71**(1–3), pp. 2163–2166.
[24] Özyılmaz, A. T., Erbil, M., and Yazıcı, B., 2005, "The Influence of Polyaniline (PANI) Top Coat on Corrosion Behaviour of Nickel Plated Copper," Appl. Surf. Sci., **252**(5), pp. 2092–2100.
[25] Antonijevic, M. M., and Petrovic, M. B., 2008, "Copper Corrosion Inhibitors. A Review," Int. J. Electrochem. Sci., **3**(1), pp. 1–28.
[26] Epstein, A. J., Smallfield, J. A. O., Guan, H., and Fahlman, M., 1999, "Corrosion Protection of Aluminum and Aluminum Alloys by Polyanilines: A Potentiodynamic and Photoelectron Spectroscopy Study," Synth. Met., **102**(1–3), pp. 1374–1376.
[27] Milica, M. G., and Branimir, N. G., 2009, "Electrochemical Polymerization and Initial Corrosion Properties of Polyaniline-Benzoate Film on Aluminum," Prog. Org. Coat., **65**(3), pp. 401–404.
[28] Sathiyanarayanan, S., Azim, S. S., and Venkatachari, G., 2006, "Corrosion Resistant Properties of Polyaniline–Acrylic Coating on Magnesium Alloy," Appl. Surf. Sci., **253**(4), pp. 2113–2117.
[29] Dominis, A. J., Spinks, G. M., and Wallace, G. G., 2003, "Comparison of Polyaniline Primers Prepared With Different Dopants for Corrosion Protection of Steel," Prog. Org. Coat., **48**(1), pp. 43–49.
[30] Talo, A., Forsén, O., and Yläsaari, S., 1999, "Corrosion Protective Polyaniline Epoxy Blend Coatings on Mild Steel," Synth. Met., **102**(1–3), pp. 1394–1395.
[31] Moraes, S. R., Huerta-Vilca, D., and Motheo, A. J., 2004, "Characteristics of Polyaniline Synthesized in Phosphate Buffer Solution," Eur. Polym. J., **40**(9), pp. 2033–2041.
[32] Tang, J., Jing, X., Wang, B., and Wang, F., 1988, "Infrared Spectra of Soluble Polyaniline," Synth. Met., **24**(3), pp. 231–238.
[33] Wang, T., and Tan, Y. J., 2006, "Understanding Electrodeposition of Polyaniline Coatings for Corrosion Prevention Applications Using the Wire Beam Electrode Method," Corros. Sci., **48**(8), pp. 2274–2290.
[34] Shao, Y., Huang, H., Zhang, T., Meng, G., and Wang, F., 2009, "Corrosion Protection of Mg–5Li Alloy With Epoxy Coatings Containing Polyaniline," Corros. Sci., **51**(12), pp. 2906–2915.
[35] Wang, H. X., Wang, H. X., and Xue, L., 2004, "Study of Adsorption of Industrial Oil by Expanded Graphite," Carbon Tech., **23**(5), pp. 21–23.
[36] Cao, Z. F., Xia, Y. Q., and Ge, X. Y., 2016, "Conductive Capacity and Tribological Properties of Several Carbon Materials in Conductive Greases," Ind. Lubr. Tribol., **68**(5), pp. 577–585.
[37] Ge, X. Y., Xia, Y. Q., and Shu, Z. Y., 2015, "Conductive and Tribological Properties of Lithium-Based Ionic Liquids as Grease Base Oil," Tribol. Trans., **58**(4), pp. 686–690.
[38] Ge, X. Y., Xia, Y. Q., and Feng, X., 2015, "Influence of Carbon Nanotubes on Conductive Capacity and Tribological Characteristics of Poly (Ethylene Glycol-Ran-Propylene Glycol) Monobutyl Ether as Base Oil of Grease," ASME J. Tribol., **138**(1), p. 011801.
[39] Fang, J., Xu, K., Zhu, L., Zhou, Z., and Tang, H., 2007, "A Study on Mechanism of Corrosion Protection of Polyaniline Coating and Its Failure," Corros. Sci., **49**(11), pp. 4232–4242.
[40] Sathiyanarayanan, S., Jeyaram, R., Muthukrishnan, S., and Venkatachari, G., 2009, "Corrosion Protection Mechanism of Polyaniline Blended Organic Coating on Steel," J. Electrochem. Soc., **156**(4), pp. C127–C134.
[41] Chen, Y., Wang, X. H., Li, J., Lu, J. L., and Wang, F. S., 2007, "Polyaniline for Corrosion Prevention of Mild Steel Coupled With Copper," Electrochim. Acta, **52**(17), pp. 5392–5399.
[42] Jiang, H., Li, J., and Xia, G., 2003, "A Study on Electric Polyaniline Used in Protection and Seal," China Surf. Eng., **16**(3), pp. 40–43.
[43] Chen, W. X., Li, F., Han, G., Xia, J. B., Wang, L. Y., Tu, J. P., and Xu, Z. D., 2003, "Tribological Behavior of Carbon-Nanotube-Filled PTFE Composites," Tribol. Lett., **15**(3), pp. 275–278.
[44] Zhao, Y. B., Zhao, Q. L., Zhou, J. F., and Zhang, Z. J., 1999, "The Synthesis and Tribological Properties of Polyaniline Microparticles," Chem. Res., **10**(3), pp. 13–16.
[45] Cao, Z. F., Xia, Y. Q., and Chen, J. H., 2016, "Tribological Properties of Vapor Grown Carbon Fibers as Conductive Additive in Grease," Tribology, **36**(2), pp. 137–144.